Carbohydrate Polymer Technologies and Applications 2 (2021) 100112

Contents lists available at ScienceDirect

Carbohydrate Polymer Technologies and Applications

journal homepage: www.sciencedirect.com/journal/carbohydrate-polymer-technologies-and-applications

Development of antibacterial biocomposites reinforced with cellulose nanocrystals derived from banana pseudostem

Pratiksha Shrestha [a], Muhammad Bilal Sadiq [b], Anil Kumar Anal [a,*]

[a] Department of Food, Agriculture and Bioresources, Asian Institute of Technology, Pathum Thani 12120, Thailand
[b] School of Life Sciences, Forman Christian College (A Chartered University), Lahore 54600, Pakistan

ARTICLE INFO

Keywords:
Crystalline nanocellulose
Nanocomposite
Biomaterial
Antimicrobial films

ABSTRACT

Crystalline nanocellulose (CNC) was derived from banana pseudostem using acid hydrolysis method. CNC was characterized by scanning electron microscope, Fourier transformed infrared spectroscopy and X-ray diffraction. CNC was found in nanometric dimensions (18.79 ± 5.30 nm diameter and 202.12 ± 37.43 nm length) and exhibited high degree of crystallinity (81.67%). Chitosan-CNC based antimicrobial nanocomposites films were prepared by the incorporation of tetracycline and showed well-demarcated zone of inhibition against *Staphylococcus aureus* and *Escherichia coli*. Chitosan-CNC nanocomposite films showed significantly ($p < 0.05$) high tensile strength and good swelling properties in comparison to control CNC films. This study suggests that banana pseudostem can be used as a raw material for economic production of CNC and nanocomposites for biomedical applications.

1. Introduction

Currently, about 2.1 billion metric tons of municipal solid waste is produced annually worldwide and global concern for waste management is increasing (Kaza, Yao, Bhada-Tata, & Van Woerden, 2018). Banana (*Musa sapientum* L) is one of the most abundant available fruits in tropical region and considered as an important global food crop and export commodity (Sitthiya, Devkota, Sadiq, & Anal, 2018). Annually, 115 million tons of banana is produced globally (FAOSTAT, 2018) and massive agro-industrial waste is generated from banana byproducts. The conversion of agro-industrial wastes to valuable products is really challenging and getting attention around the globe as it can minimize the environmental hazards (Hiranrangsee, Kumaree, Sadiq, & Anal, 2016; Sitthiya et al., 2018). Agricultural waste such as pseudostem of banana can be a sustainable and cheap source of biomaterials for biomedical applications.

Cellulose, a linear polymer of β-D glucose is the main constituent of cell wall in plants and cellulose chains are generally embedded in non-cellulosic matrix like hemicellulose and lignin. Therefore, it is essential to release the cellulose from non-cellulosic materials and cleaved into nanoscale dimension for its further applications (Haldar & Purkait, 2020). This can be achieved by sequence of chemical (strong alkali/acid) and/ or mechanical treatment (sonication, centrifugation, steam explosion). Cellulose is one of the most abundant and sustainable biomaterials with annual production of over 7.5×10^{10} tons in the biosphere (Habibi, 2014). The cellulose based nanomaterials have wide range of application in biomedical, packaging, coatings, cosmetics etc. (Gupta & Shukla, 2020).

Nanomaterials- based carriers in a system have shown enhanced *in vitro* and *in vivo* drug delivery (Ouyang et al., 2020). Crystalline nanocellulose (CNC) is nanomaterial of interest in developing nanocomposites for drug delivery in biomedical field because of its nano dimension, high surface area, hydrophilicity, biocompatibility and biodegradability (Hasan et al., 2020). Tetracycline is a broad-spectrum antibiotic and has been extensively used for wound healing and topical applications (Liu, Fan, Huo, Li, Liu & Li, 2021). CNC can be used as biomaterial for sustained drug delivery such as in bandage material and transdermal patches, (Galkina, Ivanov, Agafonov, Seisenbaeva & Kessler, 2015a). Chitosan is a linear polysaccharide derived from the deacetylation of chitin and it is a nontoxic biodegradable polymer with antimicrobial properties (Chein, Sadiq, & Anal, 2019). Chitosan dispersions with other bioactive compounds have been used to develop food packaging (Sheikh, Mehnaz, & Sadiq, 2021). The composite packaging films reinformed with nanomaterials have been used for the preservation of food products (Iamareerat, Singh, Sadiq & Anal, 2018). Chitosan films have poor mechanical properties, however functional

* Corresponding author.
E-mail address: anilkumar@ait.ac.th (A.K. Anal).

https://doi.org/10.1016/j.carpta.2021.100112
Received 25 April 2021; Received in revised form 27 June 2021; Accepted 29 June 2021
Available online 1 July 2021

properties of chitosan based composite films can be improved by reinforcement of CNC (HPS et al., 2016).

Plenty of research have been made on extraction of CNC from lignocellulosic waste to be used as reinforcing agent in packaging materials. To develop suitable bio-nanocomposite for packaging purpose, researchers have extracted CNC from different agro-industrial waste such as *Enteromorpha prolifer* (Kazharska et al., 2019), vine shoots (El Achaby, El Miri, Hannache, Gmouh, & Aboulkas, 2018), tobacco stem (Shi, Liu, Jiang, & Liu, 2020), rice straw (Perumal, Sellamuthu, Nambiar, & Sadiku, 2018) and palm trunk (Lamaming, Hashim, Leh, Sulaiman, & Lamaming, 2019). Sugarcane bagasse fibers, alfa fibers and algae waste have also been used to develop biocomposite films (Kassab, Hannache, & El Achaby, 2019). Banana waste have also been used to extract CNC to develop packaging films (Pereira et al., 2014). However, biomedical applications of CNC derived from banana pseudostem have not been reported yet. The current study aims for the isolation and characterization of CNC from banana pseudostem and its application in the development of antibiotic loaded CNC based antimicrobial film.

2. Material and methods

2.1. Materials

Banana pseudostems were obtained from the Agriculture Research Farm, Asian Institute of Technology (AIT), Thailand. All other chemicals used were of analytical grade and obtained from Sigma-Aldrich (St. Louis, MO, USA).

2.2. Extraction of crystalline nanocellulose from banana pseudostem

Chopped banana pseudostem chips (1–3 cm) were oven dried at 50 °C for 48 h, grounded and sieved to obtain fine (< 180 μm) powder (BPP). Extraction of CNC was conducted by following the method described by Mandal and Chakrabarty (2011) with some modifications (Fig. 1). Dried BPP was bleached with 0.7% $NaClO_2$ (w/v) with substrate loading ratio of 1:50 (Fiber: liquid) in boiling condition (100 °C) for 5 h and pH 4 was maintained. The process was followed by subsequent filtration through Whatman filter paper 1 and washing of bleached BPP with distilled water until neutral pH was attained. Thus, obtained neutral BPP was further treated with 5 % (w/v) sodium sulfite (Na_2SO_3) solution with substrate loading ratio of 2:1 (pulp: liquid) for 5 h in boiling condition.

Bleached BPP was again treated with 250 ml NaOH (17.5%, w/v) at boiling condition for 5 h, followed by subsequent washing of residue to achieve neutral pH (7). Thus, treated BPP was then air dried at room temperature (25 °C) and treated with 50 ml of dimethyl sulfoxide (DMSO) at 80 °C for 3 h using water bath (WNB 14 Memmert GmbH + Co. KG, Germany) and subsequent washing of cellulosic material till neutral pH was obtained.

Alkali treated BPP was hydrolyzed with 60% (w/v) H_2SO_4 with substrate loading (Fiber: liquid) ratio 1:20. Hydrolysis was executed in hot plate (H+P variomarg monotherm, Switzerland) at 50 °C for 5 h with continuous stirring at 600 rpm and the process was quenched by adding five times of additional distilled water to the reaction mix and cooled to 25 °C. The reaction mixture was then centrifuged for 10 min at 1000 rpm (Centrikon T-324, Kontron Instrument, Milano-Italy) and the clear supernatant fraction was discarded and the residue was further centrifuged by adding distilled water. The centrifugation temperature was maintained 10 °C throughout the operation to prevent cellulosic sediment from heating. This process was carried out until turbid supernatant was obtained and pH of suspension reached to 5. Finally, the suspension was sonicated by using ultrasonicator (UP200S, 200 W, Hielscher, Teltow, Germany) at a fixed frequency of 24 KHz for 10 min to obtain uniform and homogenized suspension.

2.3. Quantification of lignocellulosic components

Lignin, cellulose and hemicellulose contents of untreated BPP and chemically treated BPP were determined at each subsequent step of processing. The content of acid detergent fiber (ADF) was determined using AOAC standard method 973.18 (Helrick, 1990) and neutral detergent fiber (NDF) was determined using AOAC standard method 992.16 (AOAC, 1990). Lignin content of BPP was determined by treating with mixture of saturated $KMnO_4$ and lignin buffer solution (ratio 2:1) and weight loss of substrate was recorded. Cellulose content was calculated by subtracting percentage lignin from percentage of ADF. Similarly, hemicellulose was calculated by subtracting NDF % from ADF % (Sanjay, Siengchin, Parameswaranpillai, Jawaid, Pruncu & Khan, 2019).

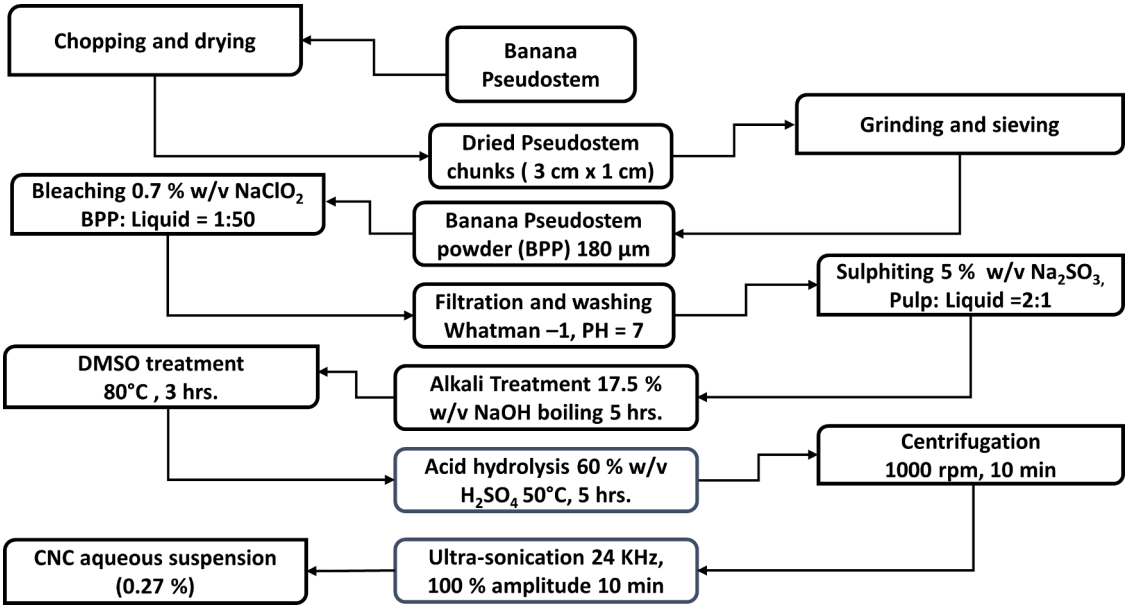

Fig. 1. Schematic diagram for the extraction of crystalline nanocellulose from banana pseudostem.

2.4. Characterization of crystalline nanocellulose

2.4.1. Scanning electron microscopy (SEM)

Morphological study of CNC was performed using field emission SEM (VERSA 3D™, FEI, USA). Aqueous solution (0.27 %) of CNC was casted into acrylic plate and oven dried to prepare thin film of CNC. The samples were then gold coated using sputtering technique and scanning electron photomicrographs were taken at an accelerated voltage (5 KV).

2.4.2. Fourier transform infrared (FTIR) spectroscopy

Fourier transform infrared (FTIR) spectra of CNC including BPP, bleached BPP and alkali treated BPP was determined using Nicolet6700 (Thermo scientific) at attenuated total reflectance (ATR) mode from 500–4000 cm^{-1}. A total of 64 scans in the range of 500–4000 cm^{-1} were recorded.

2.4.3. X- ray diffraction (XRD)

Crystallinity index of untreated fiber and CNC was determined using X-ray diffraction by using X-ray diffractometer (PANalytical X'Pert PRO, UK). Scanning was performed at 2θ range in the wide variation of 4 °–40 ° using CuKα as a source of radiation (λ = 0.1539 nm) and operating voltage of 40 KV tube voltage and 30 mA current.

2.5. Preparation of chitosan-CNC composite films

Polymer solution for composite film was prepared by following the method of Galkina, Ivanov, Agafonov, Seisenbaeva and Kessler (2015b), with some modifications (Fig. 2). The aqueous solution of butane tetra carboxylic acid (0.644 g/L), sodium hypophosphite (0.2420 g/L) and chitosan (0–5 %, w/v) were added to CNC (0.27 %, w/w) with continuous stirring at 70 °C for 2 h. The obtained solution was mixed with polyvinyl alcohol (PVA, 3 %) and further mixed for another 3 h continuously. The process was followed by subsequent addition of tetracycline (0.0131 g/L) and continuous stirring at 60 °C for 3 h.

The obtained polymer solution was developed into nanocomposite film by solution casting method as described by Chen, Lawton, Thompson & Liu (2012) with slight modifications. The polymer solution (40 mL) was poured into 6 × 6 × 2.5 mm^3 acrylic casting plates and allowed to set in vacuum dryer at 45 °C to prevent air bubbles and surface defects. The dried films were removed from casting plates after 24 h and kept in desiccator until constant weight was obtained. The prepared films were then cut into stripes (1.5×8 cm^2) to analyze the mechanical properties and cut into circular discs (2.5 cm diameter) for antibacterial assay. Each dick was loaded with 235 μg of tetracycline.

Four different nanocomposites were made using different concentrations of chitosan (0, 2, 5% w/w). The addition of chitosan above 2% was found to have undesirable swelling effect with distortion of film original shape and size. The nanocomposites with 2% chitosan showed higher stability, uniform appearance and used for the evaluation of thermal, mechanical and antibacterial properties. Control chitosan (2%) film and PVA (3%) film were also prepared by solution casting method.

2.6. Physical and mechanical properties of nanocomposite film

2.6.1. Film thickness

Thickness of nanocomposite film was determined using micrometer (Mitutoyo-Japan) with 0.01 mm sensitivity. Film thickness was measured in five different areas on the film and actual measurement was obtained by taking average.

2.6.2. Swelling index

Dried films of CNCs, PVA and chitosan were dipped into 0.02 M citrate buffer (pH 5.7) and weight of film was recorded at 15 min interval until constant weight obtained. Citrate buffer (pH 5.7) was used as wetting medium to imitate the human skin pH condition. Before taking weight, excess moisture from the film was removed by wiping with blotting paper. Swelling index was calculated using following Eq. (1) (Baskar & Kumar, 2009).

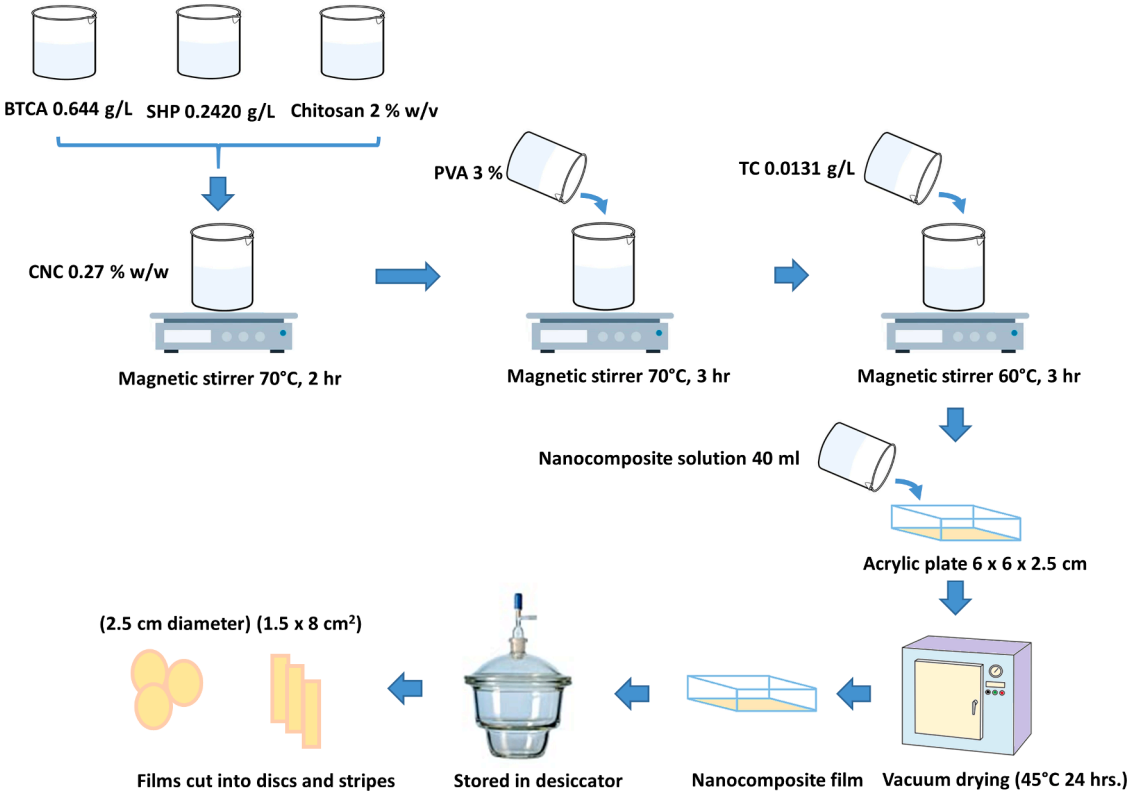

Fig. 2. Schematic diagram for preparation of Chitosan-CNC nanocomposite from nanocellulose.

$$swelling\ index\ (\%) = \frac{weight\ of\ wet\ film - weight\ of\ dry\ film}{weight\ of\ dry\ film} \times 100 \quad (1)$$

2.6.3. Tensile strength and elongation break point

Mechanical behavior of nanocomposite film was measured by using Texture Analyzer (TA.XTplus, UK) with loading cell of 500 N. Tensile strength and elongation at break were determined according to the testing method ASTM-D 882 (ASTM, 1990). The films (60 × 20 mm^2) were oven dried (50 °C for 5 h) and cooled in desiccator before analysis.

2.7. Thermo gravimetric analysis (TGA)

Thermal properties of nanocellulose and nanocomposite films were determined using LECO TGA 701(Hazel Grove, UK). The sample (1 g) was heated at increasing temperature of 20 °C/ min in nitrogen atmosphere. Volatile mass and weight loss at wide range of temperatures (30 °–900 °C) was calculated for BPP, alkali treated fiber, nanocellulose and nanocomposites.

2.8. Antibacterial activity of nanocomposite film

The antimicrobial effect of nanocomposite film was determined against *Escherichia coli* and *Staphylococcus aureus* as described by Matuschek, Brown, and Kahlmeter (2014). The bacterial strains were acquired from Thailand Institute of Scientific and Technological Research (TISTR), Bangkok, Thailand. Nanocomposite films containing chitosan (2 %, w/v), CNC (0.27 %, w/w), polyvinyl alcohol (3 %, w/v) and tetracycline (0.00131 %, w/v) were prepared by solution casting method and cut into 25 mm discs. The bacterial inoculum (10^7–10^8 CFU/ mL) was swabbed onto the surface of Mueller Hinton agar (Sigma Aldrich, USA) plate and drug loaded nanocomposite film was positioned on the center of the plate. After 18 h of incubation, each plate was examined for zone of inhibition.

2.9. Statistical analysis

One-way analysis of variance (ANOVA) and Tukey HSD tests were performed to find the significant differences among different treatments ($P < 0.05$) using statistical software package (SPSS, version 23, USA).

3. Results and discussion

3.1. Effect of chemical treatments on lignocellulosic components of BPP

Different pre-treatment steps were effective for gradual removal of cementing material of the fiber and increase in cellulosic mass throughout the treatment steps. The treatment process was able to increase the cellulosic content from 32.09 to 84.05% while hemicellulose content (31.61%) and lignin (18.57%) were reduced to less than 1 %. It was evinced that bleaching ($NaClO_2$, 0.7 W/V %) removed most of lignin (from 18.57 to 1.10 %) and some of hemicellulose (from 31.61 to 14.32 %). Since lignin is alkali soluble organic compound, bleaching decreased the percentage of lignin in treated fiber (Abraham et al., 2011). Hemicellulose was significantly decreased (from 14.32 to 1.81 %) on sulphation using sodium sulphite (Na_2SO_3, 5 W/V %) while treatment with alkali (NaOH, 17.5 W/V %) and DMSO helped in further removal of hemicellulose and lignin (Table 1). However, alkali treatment and bleaching did not alter the crystallinity of cellulose (Mahardika, Abral, Kasim, Arief, & Asrofi, 2018).

Hydrolysis removes amorphous region from cellulosic source (Zinge & Kandasubramanian, 2020). Acid hydrolysis (H_2SO_4, 60 W/V %) was able to increase the cellulose content from 67.43 to 84.05 % which indicated that besides transverse cleavage of cellulose and removal of amorphous region, acid hydrolysis was able to remove other non-cellulosic components like minerals and volatiles from lignocellulosic mass thus increasing the cellulose content. Furthermore, ultrasonication produced stable suspension and homogenous form of CNC in aqueous solution which as confirmed by Roman, Dong, Hirani, and Lee (2009).

Table 1
Treatment effects on lignocellulosic constituents of banana pseudostem powder.

Treatments	Cellulose (%)	Hemicellulose (%)	Lignin (%)
Untreated fiber	32.09 ± 0.92^a	31.61 ± 1.78^c	18.57 ± 1.63^b
Bleaching	43.69 ± 0.61^b	14.32 ± 2.41^b	1.10 ± 0.15^a
Sulphiting	53.68 ± 2.03^c	1.81 ± 0.34^a	0.88 ± 0.07^a
NaOH	63.49 ± 3.23^d	0.00 ± 0.00^a	0.56 ± 0.21^a
DMSO	67.43 ± 3.18^d	0.00 ± 0.00^a	0.15 ± 0.01^a
H_2SO_4	84.05 ± 5.79^e	0.00 ± 0.00^a	0.05 ± 0.03^a

Different superscript letters indicated significant ($p < 0.05$) differences among mean observations.

3.2. Characterization of crystalline nanocellulose

3.2.1. Morphological analysis by scanning electron microscopy

Fig. 3 (a) and (b) illustrate SEM micrograph of extracted cellulose with needle shaped structures having average diameter of 18.79 ± 5.30 nm, average length of 202.12 ± 37.43 nm and aspect ratio of 11.56 ± 3.60. The nanocellulose crystals were dispersed uniformly with no aggregation. (Mueller, Weder, & Foster, 2014) also obtained nanocellulose (width 7–70 nm and length 200–1300 nm) from banana pseudostem using chemical method. Zuluaga, Putaux, Restrepo, Mondragon and Gañán (2007) and Pereira et al., 2014 also extracted nanocellulose from banana pesudostem with diameter 5–7.2 nm and length 135–500 nm.

3.2.2. FTIR analysis of crystalline nanocellulose

Fig. 4 illustrates the FTIR spectra of CNC, alkali treated fiber, bleached fiber and untreated BPP. Presence of similar functional groups in all fiber samples justified preservation of basic chemical structure of cellulose fiber even after harsh alkali and acid treatments. The prominent spectra at 3332–3268 cm^{-1} represent stretching vibration of O-H bonds.

The asymmetric stretching vibration of aliphatic saturated C-H was observed at 2890–2917 cm^{-1}. The most obvious alteration between spectra of BPP and fibers treated chemically was the depletion of peak (1736 cm^{-1}), which was associated with the stretching of C=O bond in acetyl and uronic ester groups.

The peak at 1714 –1731 cm^{-1} was due to C=O stretching vibration of ester bond and carboxyl C=O groups in cellulosic materials (Solikhin & Murayama, 2018). Stretching vibration observed at 1608–1623 cm^{-1} was due to C=C bond in lignin whereby the absorption peak at 1623 cm^{-1} was attributed to stretching of C=C bond in benzene ring. Lignin contributed a distinguishing peak at 1432 cm^{-1} which was ascribed to methoxy –O-CH_3 group whereas, peak intensity at 1259 cm^{-1} was due to stretching of C-O-C in aryl-alkyl ether (Yang, Yan, Chen, Lee, & Zheng, 2007). Lack of all these absorption peaks from the spectra of alkali treated fibers and CNC was ascribed to removal of most of the lignin during chemical treatments.

The presence of absorption peak at 1427 cm^{-1} represented the -CH_2 symmetric bending. Absorption band at that region is also called crystalline band (Khalil, Ismail, Rozman & Ahmad, 2001). Moreover, vibration peak from 1313–1377 cm^{-1} was evinced in all samples which was due to bending vibration of C-H and C-O bonds in cellulose, hemicellulose and lignin (Le Troedec et al., 2008). The characteristics peak at 1055 cm^{-1} was designated to the presence of C-O-C stretching in the ring of Pyranose (Mandal & Chakrabarty, 2011) .

3.2.3. X- ray diffraction of crystalline nanocellulose

XRD pattern of CNC and banana pseudostem powder (BPP) is shown

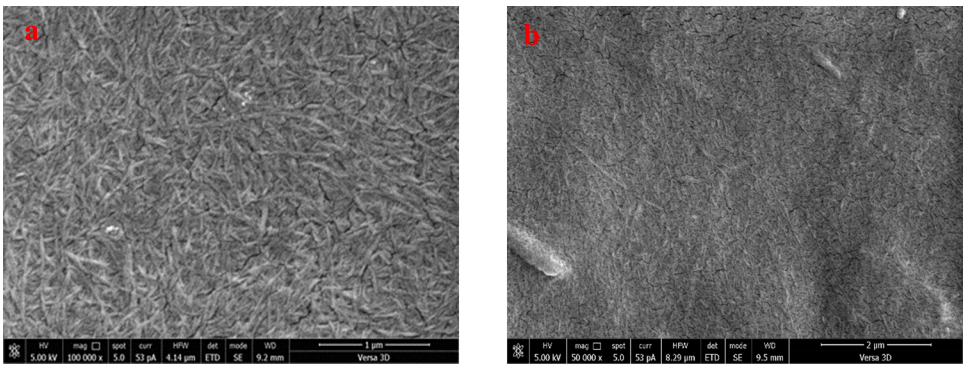

Fig. 3. Scanning electron micrograph of banana pseudostem derived crystalline nanocellulose: 100000X magnification (a), and (b) 500,000 *x* magnification.

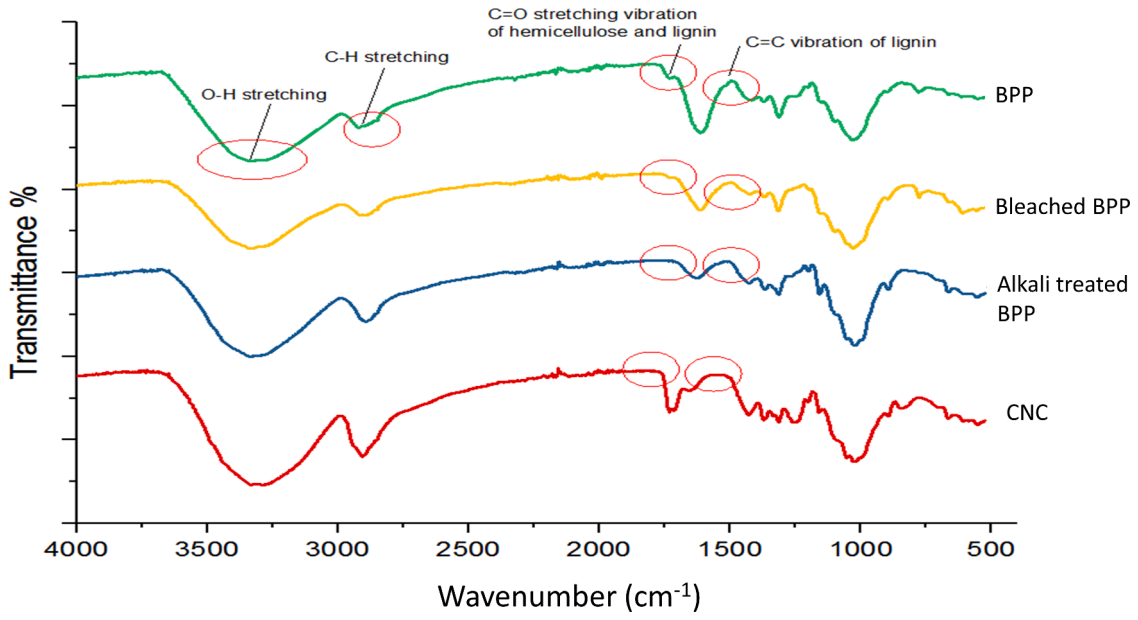

Fig. 4. Fourier transformed infrared spectroscopy of crystalline nanocellulose (CNC), banana pseudostem powder (BPP), bleached BPP and alkali treated BPP.

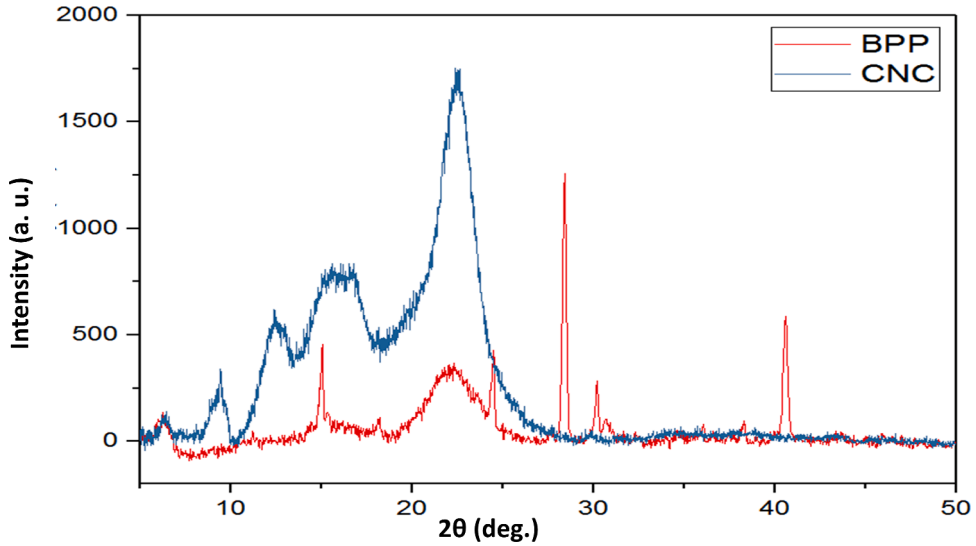

Fig. 5. X-ray diffraction analysis of crystalline nanocellulose (CNC) and banana pseudostem powder (BPP).

in Fig. 5. In diffraction pattern of CNC, prominent peaks were observed at 2θ = 15°, 16° and 22°, characteristics to the structure of native cellulose. BPP had the crystallinity index (CI) of 44.40 % while CNC exhibited CI of 81.67 %. Since, sulphuric acid exhibited ability to penetrate into amorphous regions, glycosidic bonds were cleaved under hydrolytic conditions while crystalline region remained unaffected leaving behind individual crystallites, contributing to the higher crystallinity of nanocellulose (Kargarzadeh, Ioelovich, Ahmad, Thomas, & Dufresne, 2017) .

Besides native cellulose peaks, large noise was observed in BPP indicating the presence of non-cellulosic material in the sample. Changes in peak intensity of BPP and CNCs represented the changes in crystallinity of the material. As compared to BPP, CNC had more demarcated and intensified peaks at 15° and 22° due to removal of hemicellulose and lignin by chemical treatments. Similar XRD peaks were observed for crystalline nanocellulose at 22.3° by Gupta and Raghav (2020). CNC extracted from banana pseudostem exhibited high crystallinity than the previously reported from agricultural residues such as from sweet potato (72.53 %), soya hull (73.5 %) and empty fruit bunch of palm (73–80.42%) (Lu, Gui, Zheng, & Liu, 2013).

3.3. Physical and thermal properties of CNC nanocomposite

3.3.1. Physical and mechanical properties

PVA and chitosan with more amorphous region were responsible for increasing the swelling index of nanocomposite film reinforced with CNC. Swelling index was reported to increase with the presence of more amorphous regions (Blair, Guthrie, Law, & Turkington, 1987; Chen & Hua, 1996). Swelling index of chitosan films was significantly higher than other films, which might be due to its low pH and low degree of deacetylation (Rahim, Abu, Haris & Hakim, 2016). However, swelling index of chitosan can be decreased with increase in degree of deacetylation. Swelling index of chitosan membrane prepared by 60 % degree of deacetylation was reported to be 227.6 % (Chen & Hua, 1996) . The swelling index for nanocomposite film was observed as high as 1400 % when prepared with chitosan polyvinlpyrrolidone and cellulose nanowhiskers (Hasan et al., 2017). The nanocellulose film with least swelling index was able to maintain its shape and structure with least change in dimensions while chitosan film swelled up to distortion of its shape and structure with paramount change in its dimension. However, formulation of these polymers-based nanocomposite gave a suitable fabric with no observed physical distortion in shape and size.

CNC film possessed very brittle characteristics while PVA and chitosan had a plasticizing effect on the nanocomposite film contributing final elongation at break of 2.22 ± 0.04 % (Table 2). Similar result were obtained by Lani, Ngadi, Johari, and Jusoh (2014), when CNCs 10 % (v/v) were loaded into PVA/starch blend to develop a film. However, increase in concentration of CNC in film can increase overall tensile strength of film (Rafieian & Simonsen, 2014). Chitosan films exhibited highest tensile strength (7.64 ± 0.7 MPa) and elongation at break (12.33 ± 0.08 %). Chitosan is a strong polymer exhibiting high tensile strength. The tensile strength of 16. 82 MPa was previously reported for chitosan membrane (60 % degree of deacetylation) maintained at pH 4.5 (Chen & Hua, 1996).

Table 2
Mechanical and physical properties of CNC nanocomposite, PVA film, CNC film and chitosan film.

Sample	Thickness (mm)	Swelling index(%)	Tensile strength (MPa)	% elongation at break
CNC film	0.07 ± 0.01^{a}	92.74 ± 12.9^{a}	0.21 ± 0.03^{a}	0.35 ± 0.17^{a}
PVA film	0.07 ± 0.01^{a}	165.2 ± 5.81^{c}	7.1 ± 0.9^{c}	6.68 ± 0.174^{c}
Chitosan film	0.07 ± 0.01^{a}	882.4 ± 15.36^{c}	7.64 ± 0.7^{c}	12.33 ± 0.08^{d}
Nanocomposite	0.18 ± 0.01^{b}	150.2 ± 0.78^{b}	2.64 ± 0.14^{b}	2.217 ± 0.04^{b}

Different superscript letters (a-c) indicate significant differences ($p < 0.05$) among mean observations.

3.3.2. Thermal properties

The thermal decomposition parameters were determined by the TGA curves as shown in Fig. 6. TGA analysis showed degradation steps related to moisture evaporation and pyrolysis of cellulose fiber. TGA analysis was carried out to investigate thermal stability of composite and suitability of the samples for bio-composite processing. The thermograph obtained with CNC and CNC nanocomposite showed three main weight loss regions. Initial weight loss was observed in the region 29–120 °C attributable to evaporation of water.

Second weight loss region was observed between 228–384 °C for CNCs while it was 147–263 °C for nanocomposite. This indicates slight decrease in onset of degradation temperature of nanocomposite, attributable to amorphous region from PVA and chitosan which were the main constituents of nanocomposite film. Qua, Hornsby, Sharma, Lyons, and McCall (2009) revealed that the second stage degradation mainly involves dehydration reactions and the formation of volatile products. The third stage weight loss occurred above 400 °C and involved the decomposition of carbonaceous matter (Goetz, Mathew, Oksman, Gatenholm, & Ragauskas, 2009). Weight loss of nanocomposite was observed much lower as compared to CNCs indicating chemically bound water in nanocomposite film disrupting hydrogen bond of PVA and forming new hydrogen bond with water molecules. This was attributed to plasticity and decreased polymer crystallinity in nanocomposite, indicating its suitability for developing pliable film. Similar behavior of weight loss and degradation in CNC obtained from *Citrus limetta* albedo was reported by Gupta and Raghav (2020), where degradation temperature was recorded between 165 °C–390 °C.

3.4. Antibacterial activity of nanocomposite film

The effectiveness of tetracycline loaded CNC nanocomposite was measured as zone of inhibition against test pathogens. The diameter of zone of inhibition shown by tetracycline loaded nanocomposite was found to be 36.3 ± 0.6 mm against *E. coli* and 39.3 ± 0.6 mm against *S. aureus* (Fig. 7). The control CNC and chitosan films did not show antimicrobial activity against any of the test pathogen. This study showed more promising results than previous study reported by Shao et al. (2016) where bacterial cellulose composite saturated with 0.5 g/L of tetracycline was able to give zone of inhibition 45.7 mm for *E. coli* and *38.5* mm for *S. aureus*. CNC nanocomposites can be used as carrier for transdermal drug delivery and controlled drug release (Li et al., 2019; Paulo, das Neves, & Ferreira, 2011). Nanocellulose obtained from sulfuric acid hydrolysis method resulted in negatively charged nanocellulose (Kamel, 2007) and tetracycline drug was easily attached to negatively charged CNC surface (Karimian et al., 2019). This explains that CNC nanocomposite exhibits the property of carrying tetracycline drug without being deformed and allowing its effective release. The antibacterial mechanism of tetracycline loaded nanocomposite was associated with the release of tetracycline and its adsorption onto the surface of bacterial cells by electrostatic attraction. Tetracycline disrupted the bacterial cell membrane and released the intracellular constituents, which resulted in bacterial cell death and appearance of inhibition zone around the nanocomposite films (Walsh, 2000).

4. Conclusions

The nanocellulose extraction was able to provide the rod shaped crystalline nanocellulose and the developed nanocomposite film displayed good mechanical strength, depicting the composite to be strong and flexible enough for practical applications. Antibacterial properties

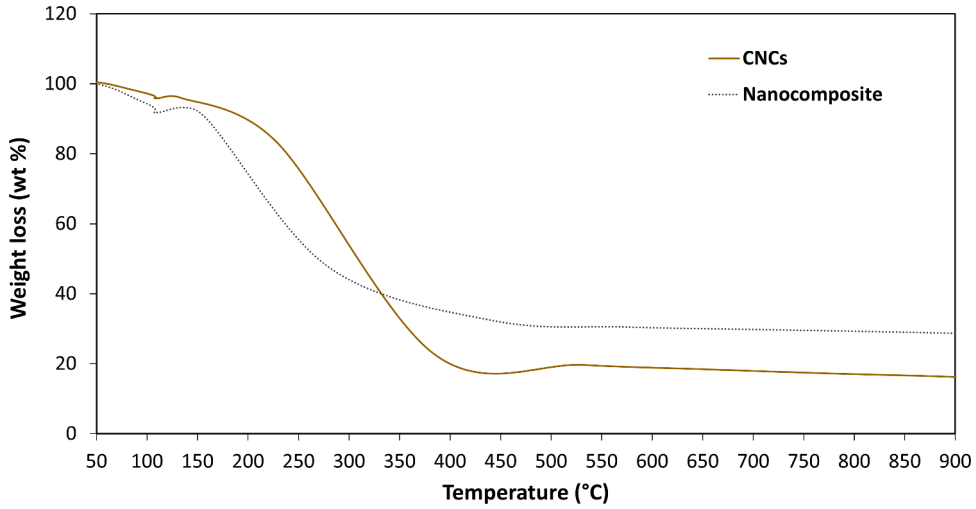

Fig. 6. Thermo Gravimetric analysis (TGA) of CNC and nanocomposite film reinforced with CNC.

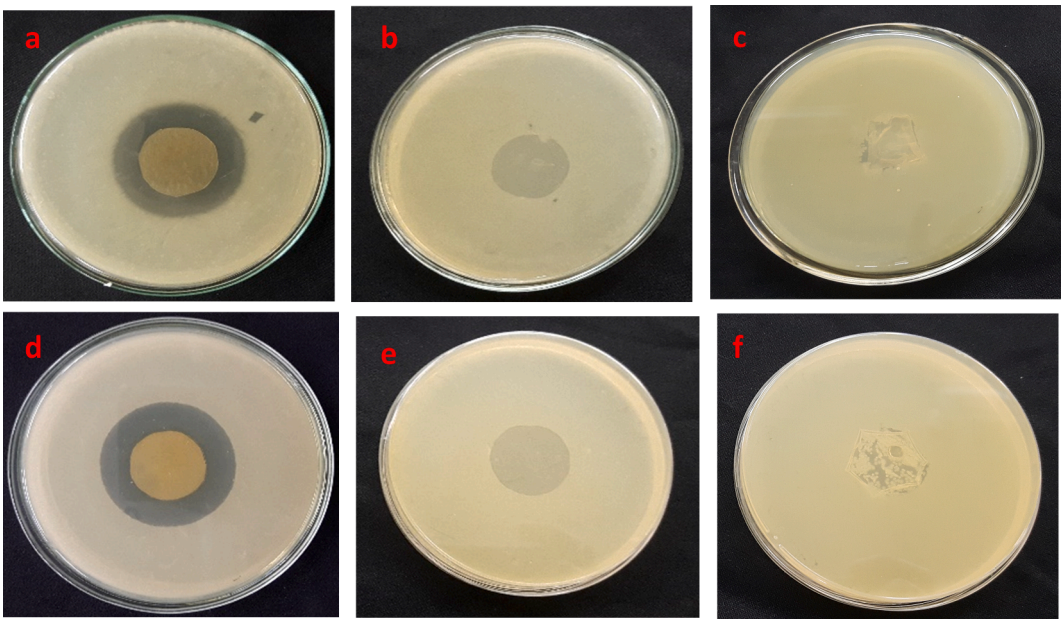

Fig. 7. Antibacterial activities of tetracycline loaded nanocomposite film against *S. aureus* (a) and *E. coli* (b), CNC control film against *S. aureus* (b) and *E. coli* (e) and chitosan control films against *S. aureus* (c) and *E. coli* (f).

of nanocomposite showed well demarcated zone of inhibition against *E. coli* and *S. aureus*. This study suggests that waste or byproducts such as banana pseudostem from banana processing industry can be utilized to obtain crystalline nanocellulose for the development of nanocomposite biomaterials for medicinal applications.

Declaration of Competing Interest

The authors declare no conflict of interest

Funding

This research did not receive any specific grant from funding agencies in the public, commercial, or not-for-profit sectors

References

Abraham, E., Deepa, B., Pothan, L. A., Jacob, M., Thomas, S., Cvelbar, U., et al. (2011). Extraction of nanocellulose fibrils from lignocellulosic fibres: a novel approach. *Carbohydrate Polymers, 86*(4), 1468–1475. https://doi.org/10.1016/j.carbpol.2011.06.034.

A. AOAC (1990). method 992.16-total dietary fiber-enzymatic gravimetric method. Official methods of analysis of association of official analytical chemists (Gaithersberg. cd)(18th cd.). association of official analytic chemists, MD, USA.

I. ASTM (1990). Annual book of American standard testing methods.

Baskar, D., & Kumar, T. S. S. (2009). Effect of deacetylation time on the preparation, properties and swelling behavior of chitosan films. *Carbohydrate Polymers, 78*(4), 767–772.

Blair, H. S., Guthrie, J., Law, T., & Turkington, P. (1987). Chitosan and modified chitosan membranes I. preparation and characterisation. *Journal of Applied Polymer Science, 33*(2), 641–656.

Chein, S. H., Sadiq, M. B., & Anal, A. K. (2019). Antifungal effects of chitosan films incorporated with essential oils and control of fungal contamination in peanut kernels. *Journal of Food Processing and Preservation, 43*(12), e14235.

D. Chen, D. Lawton, M. R. Thompson, & Q. Liu (2012). Biocomposites reinforced with cellulose nanocrystals derived from potato peel waste. Carbohydrate Polymers, 90 (1), 709–716. https://doi.org/ 10.1016/j.carbpol.2012.06.002.

Chen, R. H., & Hua, H. (1996). Effect of N-acetylation on the acidic solution stability and thermal and mechanical properties of membranes prepared from different chain flexibility chitosans. *Journal of Applied Polymer Science, 61*(5), 749–754.

El Achaby, M., El Miri, N., Hannache, H., Gmouh, S., & Aboulkas, A. (2018). Production of cellulose nanocrystals from vine shoots and their use for the development of

nanocomposite materials. *International Journal of Biological Macromolecules, 117*, 592–600.
FAOSTAT. (2018). http://www.fao.org/faostat/en/#data/QC.
Galkina, O. L., Ivanov, V. K., Agafonov, A. V., Seisenbaeva, G. A., & Kessler, V. G. (2015b). Cellulose nanofiber-titania nanocomposites as potential drug delivery systems for dermal applications. *Journal of Materials Chemistry B, 3*(8), 1688–1698.
Galkina, O. L., Ivanov, V. K., Agafonov, A. V., Seisenbaeva, G. A., & Kessler, V. G. (2015a). Cellulose nanofiber-titania nanocomposites as potential drug delivery systems for dermal applications. *Journal of Materials Chemistry B, 3*(8), 1688–1698. https://doi.org/10.1039/c4tb01823k. https://doi.org/.
Goetz, L., Mathew, A., Oksman, K., Gatenholm, P., & Ragauskas, A. J. (2009). A novel nanocomposite film prepared from crosslinked cellulosic whiskers. *Carbohydrate Polymers, 75*(1), 85–89. https://doi.org/10.1016/j.carbpol.2008.06.017. https://doi.org/.
Gupta, G. K., & Shukla, P. (2020). Lignocellulosic biomass for the synthesis of nanocellulose and its eco-friendly advanced applications. *Frontiers in Chemistry, 8*, 1203.
Gupta, R. D., & Raghav, N. (2020). Nano-crystalline cellulose: Preparation, modification and usage as sustained release drug delivery excipient for some non-steroidal anti-inflammatory drugs. *International Journal of Biological Macromolecules, 147*, 921–930.
Habibi, Y. (2014). Key advances in the chemical modification of nanocelluloses. *Chemical Society Reviews, 43*(5), 1519–1542. https://doi.org/10.1039/c3cs60204d. https://doi.org/.
Haldar, D., & Purkait, M. K. (2020). Micro and nanocrystalline cellulose derivatives of lignocellulosic biomass: A review on synthesis, applications and advancements. *Carbohydrate Polymers*, Article 116937.
Hasan, A., Waibhaw, G., Tiwari, S., Dharmalingam, K., Shukla, I., & Pandey, L. M. (2017). Fabrication and characterization of chitosan, polyvinylpyrrolidone, and cellulose nanowhiskers nanocomposite films for wound healing drug delivery application. *Journal of Biomedical Materials Research Part A, 105*(9), 2391–2404.
Hasan, N., Rahman, L., Kim, S. H., Cao, J., Arjuna, A., Lallo, S., et al. (2020). Recent advances of nanocellulose in drug delivery systems. *Journal of Pharmaceutical Investigation, 50*, 553–572.
K. Helrick (1990). AOAC method 973.18-fiber (acid detergent) and lignin in animal feeds. Official Method of Analysis of the Association of Official Analytical Chemists, 82.
Hiranrangsee, L., Kumaree, K. K., Sadiq, M. B., & Anal, A. K. (2016). Extraction of anthocyanins from pericarp and lipids from seeds of mangosteen (Garcinia mangostana L.) by Ultrasound-assisted extraction (UAE) and evaluation of pericarp extract enriched functional ice-cream. *Journal of food science and Technology, 53*(10), 3806–3813.
HPS, Abdul Khalil., Saurabh, C. K., Adnan, A. S., Fazita, M. N., Syakir, M. I., Davoudpour, Y., et al. (2016). A review on chitosan-cellulose blends and nanocellulose reinforced chitosan biocomposites: Properties and their applications. *Carbohydrate polymers, 150*, 216–226.
Iamareerat, B., Singh, M., Sadiq, M. B., & Anal, A. K. (2018). Reinforced cassava starch based edible film incorporated with essential oil and sodium bentonite nanoclay as food packaging material. *Journal of food science and technology, 55*(5), 1953–1959.
Kamel, S. (2007). Nanotechnology and its applications in lignocellulosic composites, a mini review. *Express Polymer Letters, 1*(9), 546–575.
Kargarzadeh, H., Ioelovich, M., Ahmad, I., Thomas, S., & Dufresne, A. (2017). Methods for extraction of nanocellulose from various sources. *Handbook of nanocellulose and cellulose nanocomposites* (p. 1).
Karimian, A., Parsian, H., Majidinia, M., Rahimi, M., Mir, S. M., Kafil, H. S., et al. (2019). Nanocrystalline cellulose: Preparation, physicochemical properties, and applications in drug delivery systems. *International Journal of Biological Macromolecules, 133*, 850–859.
Kassab, Z., Hannache, H., & El Achaby, M. (2019). Isolation of cellulose nanocrystals from various lignocellulosic materials: Physico-chemical characterization and application in polymer composites development. *Materials Today Proceedings, 13*, 964–973.
Kaza, S., Yao, L., Bhada-Tata, P., & Van Woerden, F. (2018). *What a waste 2.0: a global snapshot of solid waste management to 2050*. The World Bank.
Kazharska, M., Ding, Y., Arif, M., Jiang, F., Cong, Y., Wang, H., et al. (2019). Cellulose nanocrystals derived from Enteromorpha prolifera and their use in developing bionanocomposite films with water-soluble polysaccharides extracted from E. prolifera. *International Journal of Biological Macromolecules, 134*, 390–396.
Khalil, H. P. S. A., Ismail, H., Rozman, H. D., & Ahmad, M. N. (2001). Effect of acetylation on interfacial shear strength between plant fibres and various matrices. *European Polymer Journal, 37*(5), 1037–1045. https://doi.org/10.1016/S0014-3057(00)00199-3. https://doi.org/.
Lamaming, J., Hashim, R., Leh, C. P., Sulaiman, O., & Lamaming, S. Z. (2019). Bio-nanocomposite films reinforced with various types of cellulose nanocrystals isolated from oil palm biomass waste. *Waste and biomass valorization* (pp. 1–11).
N. S. Lani, N. Ngadi, A. Johari, & M. Jusoh (2014). Isolation, characterization, and application of nanocellulose from oil palm empty fruit bunch fiber as nanocomposites. Journal of Nanomaterials, 2014. https://doi.org/ 10.1155/2014/702538.
Li, N., Zhang, H., Xiao, Y., Huang, Y., Xu, M., You, D., et al. (2019). Fabrication of cellulose-nanocrystal-based folate targeted nanomedicine via layer-by-layer assembly with lysosomal pH-controlled drug release into the nucleus. *Biomacromolecules, 20*(2), 937–948.
Y. Liu, Q. Fan, Y. Huo, M. Li, H. Liu, & B. Li (2021). Construction of nanocellulose-based composite hydrogel with a double packing structure as an intelligent drug carrier. Cellulose, 1–14, https://doi.org/ 10.1007/s10570-021-03978-5.
Lu, H., Gui, Y., Zheng, L., & Liu, X. (2013). Morphological, crystalline, thermal and physicochemical properties of cellulose nanocrystals obtained from sweet potato residue. *Food Research International, 50*(1), 121–128.
Mahardika, M., Abral, H., Kasim, A., Arief, S., & Asrofi, M. (2018). Production of nanocellulose from pineapple leaf fibers via high-shear homogenization and ultrasonication. *Fibers, 6*(2), 28.
Mandal, A., & Chakrabarty, D. (2011). Isolation of nanocellulose from waste sugarcane bagasse (SCB) and its characterization. *Carbohydrate Polymers, 86*(3), 1291–1299. https://doi.org/10.1016/j.carbpol.2011.06.030. https://doi.org/.
Matuschek, E., Brown, D. F. J., & Kahlmeter, G. (2014). Development of the EUCAST disk diffusion antimicrobial susceptibility testing method and its implementation in routine microbiology laboratories. *Clinical Microbiology and Infection, 20*(4), O255–O266.
Mueller, S., Weder, C., & Foster, E. J. (2014). Isolation of cellulose nanocrystals from pseudostems of banana plants. *RSC advances, 42*, 907–915. https://doi.org/10.1039/C3RA46390G.
Ouyang, C., Zhang, S., Xue, C., Yu, X., Xu, H., Wang, Z., et al. (2020). Precision-guided missile-Like DNA nanostructure containing warhead and guidance control for aptamer-based targeted drug delivery into cancer cells *in vitro* and *in vivo*. *Journal of the American Chemical Society, 142*(3), 1265–1277.
Paulo, C. S. O., das Neves, R. P., & Ferreira, L. S. (2011). Nanoparticles for intracellular-targeted drug delivery. *Nanotechnology, 22*(49), Article 494002.
Pereira, A. L. S., Nascimento, D. M. D., Souza Filho, M. D. S. M., Morais, J. P. S., Vasconcelos, N. F., Feitosa, J. P. A., et al. (2014). Improvement of polyvinyl alcohol properties by adding nanocrystalline cellulose isolated from banana pseudostems. *Carbohydrate Polymers, 112*, 165–172. https://doi.org/10.1016/j.carbpol.2014.05.090. https://doi.org/.
Perumal, A. B., Sellamuthu, P. S., Nambiar, R. B., & Sadiku, E. R. (2018). Development of polyvinyl alcohol/chitosan bio-nanocomposite films reinforced with cellulose nanocrystals isolated from rice straw. *Applied Surface Science, 449*, 591–602.
Qua, E. H., Hornsby, P. R., Sharma, H. S. S., Lyons, G., & McCall, R. D. (2009). Preparation and characterization of poly (vinyl alcohol) nanocomposites made from cellulose nanofibers. *Journal of Applied Polymer Science, 113*(4), 2238–2247.
Rafieian, F., & Simonsen, J. (2014). Fabrication and characterization of carboxylated cellulose nanocrystals reinforced glutenin nanocomposite. *Cellulose, 21*(6), 4167–4180.
Rahim, M., Abu, N., Haris, M., & Hakim, M. R. (2016). The effect of pH on the slow-release behaviour of 1-and 2-naphthol from chitosan film. *Cogent Chemistry, 2*(1), Article 1234345.
Roman, M., Dong, S., Hirani, A., & Lee, Y. W. (2009). *Cellulose nanocrystals for drug delivery*. ACS Publications.
Sanjay, M. R., Siengchin, S., Parameswaranpillai, J., Jawaid, M., Pruncu, C. I., & Khan, A. (2019). A comprehensive review of techniques for natural fibers as reinforcement in composites: Preparation, processing and characterization. *Carbohydrate Polymers, 207*, 108–121.
Shao, W., Liu, H., Wang, S., Wu, J., Huang, M., Min, H., et al. (2016). Controlled release and antibacterial activity of tetracycline hydrochloride-loaded bacterial cellulose composite membranes. *Carbohydrate Polymers, 145*, 114–120. https://doi.org/10.1016/j.carbpol.2016.02.065. https://doi.org/.
Sheikh, M., Mehnaz, S., & Sadiq, M. B. (2021). Prevalence of fungi in fresh tomatoes and their control by chitosan and sweet orange (Citrus sinensis) peel essential oil coating. *Journal of the Science of Food and Agriculture*. https://doi.org/10.1002/jsfa.11291.
Shi, J., Liu, W., Jiang, X., & Liu, W. (2020). Preparation of cellulose nanocrystal from tobacco-stem and its application in ethyl cellulose film as a reinforcing agent. *Cellulose, 27*(3), 1393–1406.
Sitthiya, K., Devkota, L., Sadiq, M. B., & Anal, A. K. (2018). Extraction and characterization of proteins from banana (Musa Sapientum L) flower and evaluation of antimicrobial activities. *Journal of Food Science and Technology, 55*(2), 658–666.
Solikhin, A., & Murayama, K. (2018). Enhanced properties of poly (vinyl alcohol) composite films filled with microfibrillated cellulose isolated from continuous steam explosion. *International Journal of Plastics Technology, 22*(1), 122–136.
Walsh, C. (2000). Molecular mechanisms that confer antibacterial drug resistance. *Nature, 406*(6797), 775–781.
Yang, H., Yan, R., Chen, H., Lee, D. H., & Zheng, C. (2007). Characteristics of hemicellulose, cellulose and lignin pyrolysis. *Fuel, 86*(12–13), 1781–1788. https://doi.org/10.1016/j.fuel.2006.12.013. https://doi.org/.
Zinge, C., & Kandasubramanian, B. (2020). Nanocellulose based biodegradable polymers. *European Polymer Journal*, Article 109758.
Zuluaga, R., Putaux, J. L., Restrepo, A., Mondragon, I., & Gañán, P. (2007). Cellulose microfibrils from banana farming residues: Isolation and characterization. *Cellulose, 14*(6), 585–592. https://doi.org/10.1007/s10570-007-9118-z. https://doi.org/.